Control Engineering Practice 36 (2015) 142–150

Contents lists available at ScienceDirect

Control Engineering Practice

journal homepage: www.elsevier.com/locate/conengprac

Input–output feedback linearizing control of linear induction motor taking into consideration the end-effects. Part II: Simulation and experimental results

Francesco Alonge [a], Maurizio Cirrincione [b], Marcello Pucci [c,*], Antonino Sferlazza [a,c]

[a] D.E.I.M. (Department of Energy Information Engineering and Mathematical Models), University of Palermo, Viale delle Scienze, 90128 Palermo, Italy
[b] The School of Engineering and Physics, The University of the South Pacific, Laucala Campus, Suva, Fiji
[c] I.S.S.I.A. Section of Palermo (Institute on Intelligent Systems for Automation), via Dante 12, Palermo 90128, National Research Council of Italy (CNR), Italy

ARTICLE INFO

Article history:
Received 21 October 2013
Accepted 18 August 2014
Available online 4 November 2014

Keywords:
Linear induction motor (LIM)
Feedback linearization
End-effects

ABSTRACT

This is the second part of a paper, divided in two parts, dealing with the application of the input–output feedback linearization (FL) control technique to linear induction motors (LIMs).

The first part has treated the theoretical formulation of the input–output feedback linearization control technique as to be applied to linear induction motors. This second part describes the set of tests, both in numerical simulations and experiments, performed to assess the validity of the control technique. In particular, it addresses the issues of the sensitivity of the FL control versus the LIM electrical parameters' variations and the improvements achievable by considering the LIM dynamic end effects in the control formulation.

The proposed FL technique has been further compared, under the same closed-loop bandwidths of the flux and speed systems, with the industrial standard in terms of high performance control technique: field oriented control (FOC).

1. Introduction

This is the second part of a paper, divided in two parts, dealing with the theoretical definition and application of the input-output Feedback Linearization–>input–output feedback linearization (FL) control technique to linear induction motor (LIM) drives. The first part of this paper has illustrated the theoretical framework which leads to the development of the FL controller suitable for LIM. It has also illustrated how to manage the constraints on the electrical variables arising from the adoption of the FL. The controller design criteria have been further defined.

This second part deals with the verification of the proposed FL control in both numerical simulation and experiments. It describes the experimental setup adopted for the assessment of the proposed control law. It firstly illustrates results obtained in numerical simulation in Matlab®–Simulink® environment. It further shows results connoting the improvements achievable thanks to the exploitation of the dynamic end effects in the FL controller, instead of adopting of the classic rotating induction machine (RIM) model. It also proposes a sensitivity analysis of the FL controller versus the variation of the two most significant electrical parameters of the LIM: the inductor resistance R_s and the induced part time constant T_r.

The proposed FL control has been also compared in numerical simulation with the classic FOC, with a flux model specifically developed for LIMs (Pucci, 2012), under the same closed-loop dynamic conditions.

2. Simulation results

The proposed input–output feedback linearization (FL) control technique has been verified in numerical simulation. With this regard, the entire numerical benchmark has been implemented in Matlab®–Simulink® environment.

As far as the LIM dynamic model is concerned, which is the machine under test in the following tests, the space-vector dynamic model of the LIM taking into consideration the LIM end effects (Pucci, 2012, 2014) has been implemented: this model implements the dynamic end effects by suitable speed-varying inductance and resistance terms and including also a braking force term. It offers a very reliable representation of the LIM dynamic behavior, as confirmed by Pucci (2014). The only limits of such

* Corresponding author.
E-mail addresses: francesco.alonge@unipa.it (F. Alonge), m.cirrincione@ieee.org (M. Cirrincione), pucci@pa.issia.cnr.it (M. Pucci), antonino.sferlazza@unipa.it, sferlazza@pa.issia.cnr.it (A. Sferlazza).

http://dx.doi.org/10.1016/j.conengprac.2014.09.013
0967-0661/

a model is that it does not take into consideration the LIM static end effects, which are however less significant than the dynamic ones as far as the control issues are concerned. The rated values and electrical parameters of the adopted LIM are given in Table 1.

To verify the improvement in the dynamic performance achievable with the adoption of the proposed input–output feedback linearization with respect to other control techniques in the literature, FL has been compared with the industrial standard in terms of high performance control: field oriented control (FOC). In particular, among the various FOC versions, the classic induced part flux oriented control has been adopted (equivalent to the rotor-flux-oriented control in RIMs, Leonhard, 2001; Vas, 1998). In particular, the version of FOC based on the induced part flux model written in the induced part flux reference frame taking into consideration the LIM dynamic end effects has been adopted (Pucci, 2012). This version of the FOC, specifically developed for LIMs, is certainly the best benchmark with respect to which the performance of the proposed input–output feedback linearization can be evaluated and inherently permits better dynamic performance than the standard FOC developed for RIMs and applied to LIMs.

2.1. Terms for the comparison between FL and FOC

Comparing two different control techniques is always a hard task. In general, to make a meaningful comparison, two control techniques must be compared trying to impose the same dynamic behavior of the closed loop system of the variable to be controlled. This assumption corresponds, in the case under study, to impose the same dynamics of the controlled induced part flux amplitude and machine linear speed loops, with both FL and FOC.

As far as flux control is concerned, in the FL case, defining the dynamics of the flux control corresponds to fix a set of reasonable values of gains $k_{\psi 1}$ and $k_{\psi 2}$ such that the dynamic of the closed loop equation of the flux error (52)-Part I has fixed specifics, i.e. bandwidth and phase margin. In this case, the values shown in Table 1-(Part I) have been assigned. The dynamic of the inductor current i_{sx}, in FL, is indirectly controlled. In fact the current i_{sx} is proportional to ν_{ψ} as is shown in Section 5-(Part I), so only the flux dynamic is imposed, since the current dynamic results are indirectly fixed such that the closed loop flux has the imposed dynamic.

Correspondingly, in the FOC case, the induced part flux amplitude is controlled by a PI controller (see block diagram of the FOC in Fig. 5 of Pucci, 2012). The hierarchy of the control is organized so that the output of the flux controller is the reference of the direct component of the inductor current i_{sx} in the induced part flux reference frame. The PI regulating i_{sx} has been tuned so to impose the best dynamic performance of its control loop, taking into consideration that:

(1) The transient inductance value of LIM is a speed varying quantity, differently from that of the RIM, which can be assumed to be constant. The design of the controller has been thus made for one value of the speed (the rated one typically), and then further verified at lower speeds.
(2) In the LIM case, differently from the RIM one, the dynamics of the inductor current is slower than that of the induced part flux, because of the big air-gap and thin aluminium track (Pucci, 2014). It makes flux control more critical for the LIM than for the RIM.

The entire flux loop has been then tuned, in the FOC case, so that the dynamic is equal to that imposed with the FL (see Table 1-(Part I) for the values of the proportional and integral gains given to all the controllers in the FOC case). This is confirmed by comparing the Bode diagrams of the closed loop transfer functions of the controlled induced part flux in the FL and FOC cases (Fig. 4-(Part I)). It can be easily observed that the 3 dB bandwidths and the phase margins (shown in Table 2-(Part I)) of the induced part flux in both cases are almost equal ($B_{-3db} = 455$ rad/s and $m_{\Phi} = 40^{\circ}$). Finally, even the maximum values of the acceptable inductor current amplitudes, above which the control presents a saturation action, have been set equal for FL and FOC, to make a reliable comparison.

Table 1
Parameters of the LIM.

Rated power, P_{rated} (W)	425
Rated voltage, U_{rated} (V)	380
Rated frequency, f_{rated} (Hz)	60
Pole-pairs	3
Inductor resistance, R_s (Ω)	11
Inductor inductance, L_s (mH)	637.6
Induced part resistance, R_r (Ω)	32.57
Induced part inductance, L_r (mH)	757.8
3-phase magnetizing inductance, L_m (mH)	517.5
Rated thrust, F_n (N)	62
Rated speed (m/s)	685
Mass (kg)	20

As far as speed control is concerned, in the FL case, defining the dynamics of the speed control corresponds to fix a set of reasonable values of gains k_{v1} and k_{v2} such that the dynamic of the closed loop equation of the speed error (53)-(Part I) has fixed specifics, i.e. bandwidth and phase margin. In this case, the values shown in Table 1-(Part I) have been assigned. The dynamic of the inductor current i_{sy}, in FL, is indirectly controlled. In fact the current i_{sy} is function of a as is shown in Section 5-(Part I), so only the speed dynamic is imposed, since the current dynamic results indirectly fixed such that the closed loop speed have the imposed dynamic.

Correspondingly, in the FOC case, the speed is controlled by a PI controller (see block diagram of the FOC in Fig. 5 of Pucci, 2012). The hierarchy of the control is organized so that the output of the speed controller is reference of the quadrature component of the inductor current i_{sy} in the induced part flux reference frame. The parameters of the PI regulating i_{sy} have been tuned equal to those of i_{sx}.

The entire speed loop has been then tuned, in the FOC case, so that the dynamic is equal to that imposed with the FL (see Table 1-(Part I) for the values of the proportional and integral gains given to all the controllers in both the FL and FOC cases). This is confirmed by comparing the Bode diagrams of the closed loop transfer function of the speed loops in the FL and FOC cases (Fig. 5-(Part I)). It can be easily observed that the 3 dB bandwidths and the phase margins (shown in Table 2-(Part I)) of the speed in both cases are almost equal ($B_{-3db} = 37$ rad/s and $m_{\Phi} = 128^{\circ}$).

It should be however borne in mind that, while the FL ensures that the poles of the induced part flux and speed are always those imposed by the designer, independently from the working speed of the LIM, in the FOC case their dynamics are imposed by the designer for one working condition (rated speed where the end effects are more visible), while they then vary with the speed of the machine. This results in the degradation of the performance of FOC with respect to FL, as shown in the following.

2.2. Comparative tests

Even the choice of the tests under which the FL has to be compared to the FOC is not straightforward. As clearly demonstrated in Marino, Peresada, and Valigi (1993) and Marino, Tomei, and Verrelli (2010) for the RIM case, and verified theoretically in the Part I of this paper for the LIM case, the major differences between FOC and FL control appear when the machine is

controlled with a varying flux level, since during this working condition there is a coupling effect between the flux and speed controls caused by the presence of flux term in the speed equation. Moreover in LIM case the coupling effects are present also at constant flux because the parameters in the flux equation are time-varying with the speed due to the end-effects. A meaningful comparison between the FL and FOC can be therefore made under varying flux amplitude working conditions. This is not an usual drive working condition since, below the rated speed of the motor, an electrical drive is usually regulated at constant flux so to maintain the full force capability.

There are only two working conditions in which varying the flux level of the motor is convenient:

(1) *Field weakening*: In this case, flux reduction is necessary to permit the available voltage to counterbalance the back EMF (ElectroMotrice force) at increasing speed.
(2) *Minimum losses (maximum efficiency) operation*: In this case, at lower loads, the flux level is usually reduced to permit the losses to be minimized. If the load force varies with the speed, a contemporary variation of the flux level and speed (force) thus occurs.

On the basis of the above, the working conditions (1) and (2) have been chosen to compare FL and FOC.

2.3. Results

As a first test, a speed step from 0 to 10 m/s in the field weakening region (rated speed of the LIM is 6.8 m/s) has been given to the LIM drive, followed by a speed reversal at no load in the field weakening region, from 10 to −10 m/s. This is a particularly challenging test, since during the reversal, not only the flux varies with the force and the speed, but also the electrical parameters of the LIM vary continuously because of its dynamic end effects. Figs. 1 and 5 show the LIM reference and measured speed, obtained respectively with the FL and the FOC, under this test. Figs. 2 and 6 show the corresponding waveforms of the reference and real induced part flux amplitudes, obtained respectively with the FL and the FOC. Figs. 3 and 7 show the corresponding waveforms of the electromagnetic, braking and net thrust as well as the load force, obtained respectively with the FL and the FOC. Finally, Figs. 4 and 8 show the corresponding waveforms of the inductor phase currents, obtained respectively with the FL and the FOC.

These figures show that both control technologies work properly, even under these challenging working conditions, as expected. As far as the speed is concerned, FL permits the speed reversal to be accomplished in a lower time than the FOC (3.86 s in

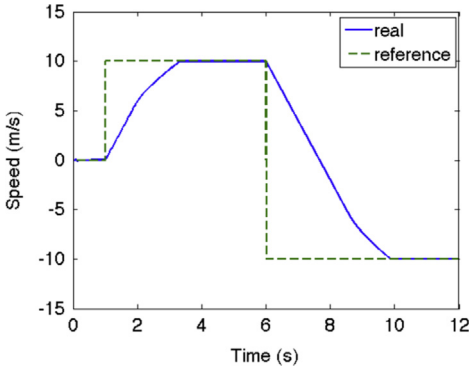

Fig. 1. Reference and measured speed during the speed step variations 0→10→−10 m/s (FL).

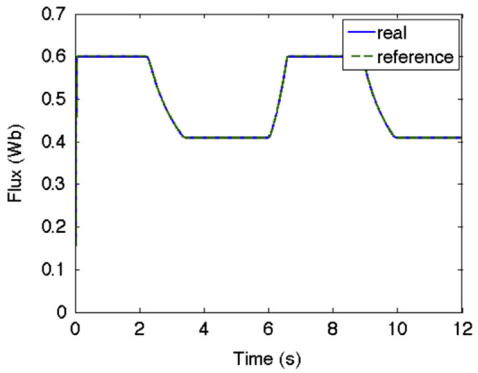

Fig. 2. Reference and real induced part flux amplitude during the speed step variations 0→10→−10 m/s (FL).

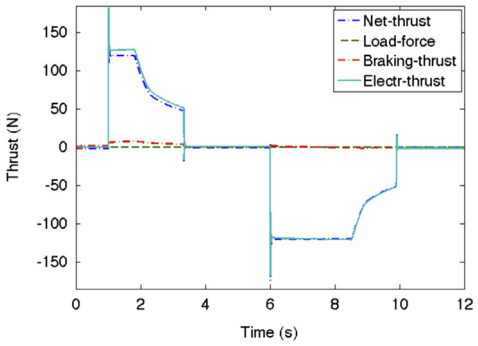

Fig. 3. Electromagnetic, braking, net thrust and load force during the speed step variations 0→10→−10 m/s (FL).

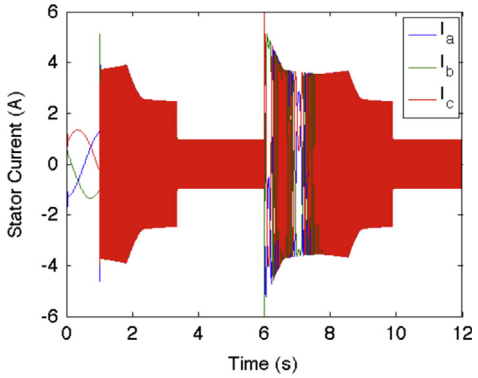

Fig. 4. Inductor phase currents during the speed step variations 0→10→−10 m/s (FL).

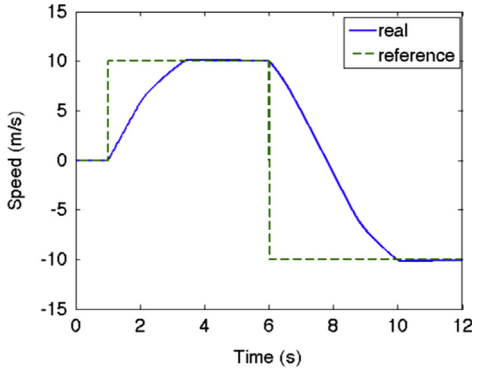

Fig. 5. Reference and measured speed during the speed step variations 0→10→−10 m/s (FOC).

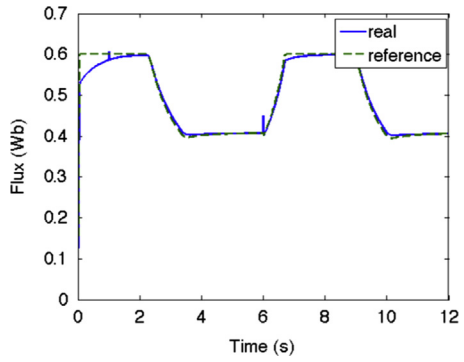

Fig. 6. Reference and real induced part flux amplitude during the speed step variations 0→10→−10 m/s (FOC).

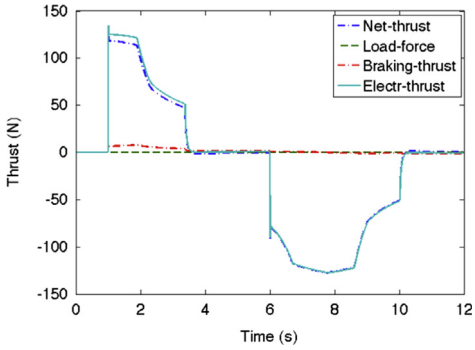

Fig. 7. Electromagnetic, braking, net thrust and load force during the speed step variations 0→10→−10 m/s (FOC).

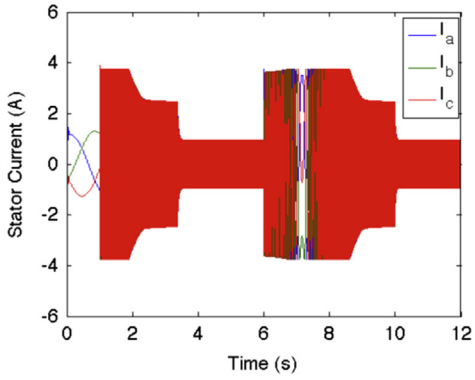

Fig. 8. Inductor phase currents during speed step variations 0→10→−10 m/s (FOC).

the FL case versus 3.97 s in the FOC case, which is 3.2% lower). This is confirmed also by the computation of the Integral Absolute Error (IAE) performance index (see Table 2), equal to 43 for the FL and 46 for the FOC, which is almost 7% lower.

As far as the flux is concerned, it should be noted that, in both cases, whenever the speed overcomes the rated value, the flux controller commands a reduction of it (see block diagram in Fig. 6-(Part I)). During the constant speed region, the flux is regulated at its minimum value, as expected. These figures clearly show that the real flux tracks the reference one much better in the FL than in the FOC case. This is confirmed also by the computation of the IAE performance index (see Table 2), equal to 6×10^{-3} for the FL and 0.081 for the FOC, which is almost 1250% lower. In general, a better flux control is observable with the FL than with the FOC.

As far as the thrust is concerned, these figures show that both FL and FOC permit a very fast thrust control. However, during the

Table 2
Performance indicators.

Test description	$e_v=v_{ref}-v$	$e_\psi=\psi_{ref}-\psi_r$	$e_F=F_r-F_e$
FL			
Test at 10 m/s (no-load)	IAE=43	$IAE=6\times10^{-3}$	IAE=N.A.
	ITAE=N.A.	ITAE=N.A.	ITAE=N.A.
Test at 0.5 m/s (load 100 N m)	$IAE=2.5\times10^{-3}$	$IAE=5.1\times10^{-3}$	IAE=1
	$ITAE=6\times10^{-3}$	$ITAE=3\times10^{-3}$	ITAE=0.025
Test at 5 m/s (load 100 N m)	$IAE=4\times10^{-3}$	$IAE=6.4\times10^{-3}$	IAE=1.25
	$ITAE=3\times10^{-3}$	$ITAE=3\times10^{-3}$	ITAE=0.045
FOC			
Test at 10 m/s (no-load)	IAE=46	IAE=0.081	IAE=N.A.
	ITAE=N.A.	ITAE=N.A.	ITAE=N.A.
Test at 0.5 m/s (load 100 N m)	IAE=0.35	IAE=0.03	IAE=6.5
	ITAE=0.5	ITAE=0.016	ITAE=5.3
Test at 5 m/s (load 100 N m)	IAE=0.33	IAE=0.03	IAE=6.8
	ITAE=0.52	ITAE=0.016	ITAE=5.2

The IAE index is defined as $IAE=\int_{t_0}^{\infty}|e(t)|\,dt$.
The ITAE index is defined as: $ITAE=\int_{t_0}^{\infty}t|e(t)|\,dt$.

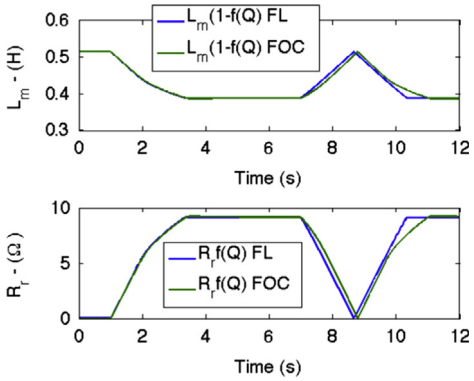

Fig. 9. Parameters $\hat{L}_m=L_m(1-f(Q))$ and $\hat{R}_r=R_rf(Q)$ during the test in Figs. 1– 8.

first instants of the speed reversal, when the force is commanded instantaneously to its maximum value and correspondingly the flux starts to be reduced, the FL is able to control immediately the net force to its maximum constant value, while FOC shows a small time interval in correspondence to which the net force is lower than its maximum, since it is not able to instantaneously exploit flux and thrust variations. In this case the FL exhibits a better dynamic performance, as expected.

As far as the inductor current amplitude is concerned, the FL shows an amplitude varying during the speed transient, while the FOC shows constant current amplitudes. This can be explained evaluating that FL exploits better the LIM, being able to linearize and decouple instantaneously its model even during transients.

Fig. 9 shows the speed varying electrical parameters $\hat{L}_m=L_m(1-f(Q))$ and $\hat{R}_r=R_rf(Q)$ of the LIM during this test. It is clearly observable that the higher the LIM speed, the higher is the value of $\hat{R}_r=R_rf(Q)$ and the lower the value of $\hat{L}_m=L_m(1-f(Q))$, as expected, according to the above described model.

As a second set of tests, the LIM drive has been operated at constant speed, respectively at nominal speed (5 m/s) and low speed (0.5 m/s) and a step load force variation of 100 N has been applied simultaneously to a flux variation (from 0.2 Wb to 0.6 Wb). This kind of test emulates a behavior of the LIM drive during a minimum losses transient operation.

Fig. 10 shows the LIM reference and measured speed during these two tests, highlighting the direct comparison of the related curves in the FL and FOC cases. Fig. 11 shows the corresponding waveforms of

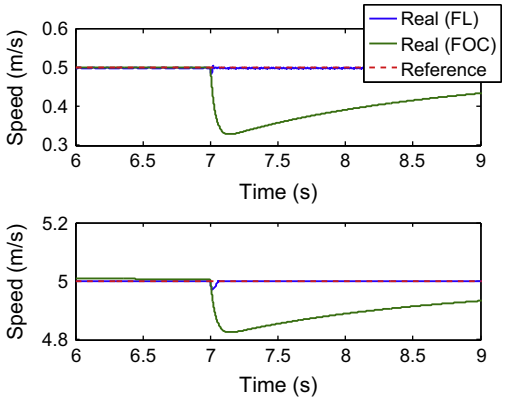

Fig. 10. Reference and real speed during a simultaneous load (0→100 N) and flux (0.2→0.6 Wb) variations at constant speed of 0.5 m/s and 5 m/s.

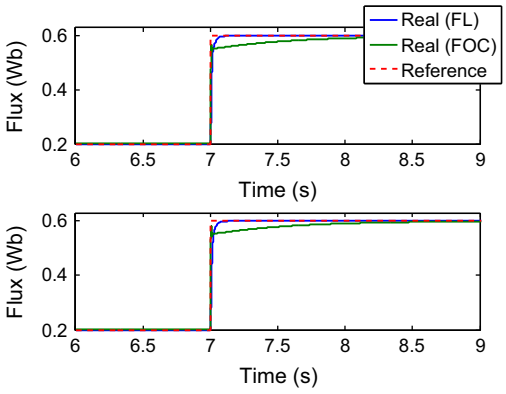

Fig. 11. Reference and real induced part flux amplitude during a simultaneous load (0→100 N) and flux (0.2→0.6 Wb) variations at constant speed of 5 m/s and 0.5 m/s.

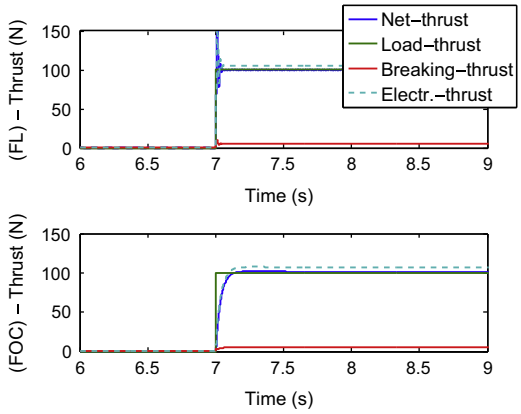

Fig. 12. Electromagnetic, braking, net thrust and load force during a simultaneous load (0→100 N) and flux (0.2→0.6 Wb) variations at constant speed of 0.5 m/s (FOC) and (FL).

the reference and real induced part flux amplitudes, obtained respectively with the FL and the FOC. Finally Figs. 12 and 13 show the corresponding waveforms of the electromagnetic, braking and net thrust as well as the load force, obtained respectively with the FL and the FOC.

Both control techniques exhibit high performance in the load force rejection during contemporary load and flux variations. In particular, it is clear from figures that flux control is much faster with FL than with FOC under these working conditions, as expected. Correspondingly, even if both controls properly reject

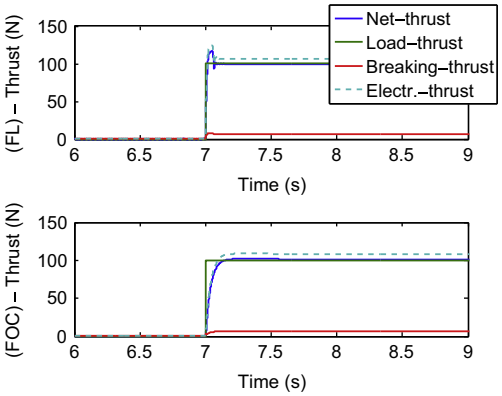

Fig. 13. Electromagnetic, braking, net thrust and load force during a simultaneous load (0→100 N) and flux (0.2→0.6 Wb) variations at constant speed of 5 m/s (FOC) and (FL).

load step variations, the net thrust increase to the load step is much faster in the FL case as witnessed by the settlement times: 0.17 s (0.14 s) in FL versus 4 s (3.8 s) in FOC in the 5 m/s (0.5 m/s) test. As a result, speed control after load force application is much faster with FL than with FOC, and this is particularly evident during the test at low speed, as witnessed by the speed waveforms.

The result of these comparisons is given in Table 2, providing the IAE and Integral Time-weighted Absolute Error (ITAE) performance indexes of the flux, speed and thrust starting from the load insertion instant. The analysis of the IAE index shows that FL permits an IAE of the flux loop 5.9 times (4.7 times) lower than FOC for the test at 0.5 m/s (5 m/s), an IAE of the speed loop 330 times (140 times) lower than FOC for the test at 0.5 m/s (5 m/s), and an IAE of the thrust (even if not directly controlled) 6.5 times (5.4 times) lower than FOC for the test at 0.5 m/s (5 m/s). Same kind of conclusions can be made from the analysis of the ITAE index. The ITAE index in some tests is not available (N.A.) since there is not a unique transient (i.e. there are multiple steps).

3. Influence of the LIM model accuracy on the FL performance

The capability of the FL control to properly work, guaranteeing high dynamic performance and decoupled control of the induced part flux and thrust of the LIM, depends on the correct knowledge of the LIM model. With this regard, there are two main potential sources of error influencing the dynamic performance of the FL controller: (1) the correct knowledge of the LIM model formulation, (2) the correct knowledge of the electrical parameters of the adopted model. The influence of both sources of error on the FL control action has been analyzed in numerical simulation. The LIM model adopted as machine under test is a recently developed space-vector dynamic model taking into consideration the LIM dynamic end effects (Pucci, 2014).

3.1. Influence of the electrical parameters variation

To verify the effects of the variations of the electrical parameters on the dynamic performance the flux and speed loops as obtained with the FL, the modification of two among its most significant parameters has been taken into consideration: the inductor resistance (R_s) and the induced part time constant (T_r). In the simulation results shown above, the values given to electrical parameters of the LIM (see Table 1), have been identified by a suitable off-line parameters estimation technique as in Alonge, Cirrincione, D'Ippolito, Pucci, and Sferlazza (2014). These

values have been considered in the following tests, the true values of the parameters.

Starting from these values, both R_s and T_r of the machine under test have been changed simultaneously as much as 5% up to 30% with respect to their initial values. In each test, while the parameters of the LIM have been assumed to vary, the corresponding parameters adopted by the FL controller have been kept constant at their true values. At the same time, the corresponding parameters adopted by the flux model (in this case depending only on T_r) have been varied accordingly to the variation of the LIM parameters. This has been purposely made so to consider the effects of the parameters variations only on the FL control action. If the flux model parameters were maintained constant, while the LIM parameters varying, there would have been a further source of error on the control action caused by the detuning of the flux model, leading to a wrong estimation of both the amplitude and phase of the induced part flux space vector, with corresponding incorrect condition of field orientation. This further source of error would have masked the effect of the parameters mismatch on the FL control action. As a result, Table 3 shows the IAE and ITAE control performance indexes for different values of the percent modification given contemporary to R_s and T_r, as obtained during two start-up tests with a simultaneous step variations of the induced part flux from 0.2 to 0.6 Wb and speed from 0 to 0.5 m/s and from 0 to 5 m/s.

It can be clearly observed that both IAE and ITAE indexes increase, almost linearly, with the percent variation of the parameters. This is to be expected, since the worse the knowledge of the LIM parameters, the worse are to be expected the dynamic performance of both the speed and flux control loops. It is noteworthy also that both indexes are higher in the test at high speed (5 m/s) than in the test at low speed (0.5 m/s), for each value of the parameters variation. This is also to be expected, since the higher the LIM speed step amplitude the higher is the duration of the transient and therefore the effect on the control action of the parameters mismatch. Finally, the rate of change of the ITAE index is always bigger than that of the IAE, for both the flux and the speed loops, meaning that the parameters mismatch is a cause of a significant worsening of the steady-state behavior of the control in both the flux and speed loops.

Table 3
IAE and ITAE control performance indexes of the speed and flux loops versus the % variations of R_s and T_r for a 0.2→0.6 Wb flux and 0→5 m/s, 0→0.5 m/s speed steps.

Test description	$e_v = v_{ref} - v$	$e_w = \psi_{ref} - \psi_r$
Test at 5 m/s *at-load*		
5% R_s R_r variation	IAE=0.0046	IAE=0.0210
	ITAE=0.0091	ITAE=0.0394
10% R_s R_r variation	IAE=0.0082	IAE=0.0360
	ITAE=0.0182	ITAE=0.0772
15% R_s R_r variation	IAE=0.0118	IAE=0.0515
	ITAE=0.0273	ITAE=0.1163
20% R_s R_r variation	IAE=0.0154	IAE=0.0676
	ITAE=0.0364	ITAE=0.1567
25% R_s R_r variation	IAE=0.0190	IAE=0.0842
	ITAE=0.0455	ITAE=0.1986
30% R_s R_r variation	IAE=0.0226	IAE=0.1014
	ITAE=0.0546	ITAE=0.2422
Test at 0.5 m/s *at-load*		
5% R_s R_r variation	IAE=0.0036	IAE=0.0135
	ITAE=0.0085	ITAE=0.0216
10% R_s R_r variation	IAE=0.0070	IAE=0.0221
	ITAE=0.0170	ITAE=0.0433
15% R_s R_r variation	IAE=0.0104	IAE=0.0308
	ITAE=0.0255	ITAE=0.0656
20% R_s R_r variation	IAE=0.0137	IAE=0.0398
	ITAE=0.0339	ITAE=0.0885
25% R_s R_r variation	IAE=0.0171	IAE=0.0491
	ITAE=0.0424	ITAE=0.1120
30% R_s R_r variation	IAE=0.0205	IAE=0.0585
	ITAE=0.0509	ITAE=0.1361

Fig. 14 shows the steady-state tracking errors of the flux, obtained with FL, versus the percent variations of R_s and T_r during the two speed step references of 0.5 m/s and 5 m/s. It clearly shows that the steady state error increases with the percent variation of the parameters, but it remains contained in a small range. Same considerations cannot be done for the speed because the feedback loop is closed using the measured speed.

In conclusions, it can be finally stated that even in presence of significant simultaneous variations of R_s and T_r, up to 30% of their rated values, the control system remains stable and the behavior of the controller, in terms of both transient and steady-state, does not degrade significantly so to invalidate its proper adoption.

3.2. *Influence of the LIM dynamic end effect on the FL performance*

To verify the improvements arising from considering the LIM dynamic end effects in the theoretical formulation of the FL control, the FL control technique has been applied to the LIM drive twice, respectively as explained in Part I of this paper, and afterwards imposing $f(Q)=0$ in the FL control (no end effects); it corresponds to the adoption of the FL developed for RIMs (De Luca & Ulivi, 1989; Krzeminski, 1987; Kim, Ha, & Ko, 1990; Marino et al., 1993, 2010). In both cases, as machine under test the dynamic model of the LIM taken into consideration the end effects developed in Pucci (2014) has been adopted. To assess these improvements, a flux reference of 0.6 Wb has been given to the LIM drive and afterwards a reference of speed of 10 m/s has been provided : this causes the drive to work in the field-weakening region, since the rated speed of the motor is 6.8 m/s. This test is particularly challenging, since it corresponds to a sudden variation of the flux and speed at high speed, where the dynamic end effects are more visible. Fig. 15 shows the reference and real flux of the LIM, respectively obtained with FL including the end effects and not including them. Fig. 16 shows the corresponding waveform of the reference and real speed of the LIM, respectively obtained with FL including the end effects and not including them. It can be easily observed that, while FL considering the end effects permit the real machine flux to track always the reference, when end effects are not accounted for, there is a time interval (during the speed transient), in which the real flux deviates the reference, leading to a steady-state tracking error on the flux control.

As far as the speed waveform is concerned, it can be easily noticed that below the rated speed of the LIM, the performance of FL with and without considering the end effects are almost equal; for working speeds above the rated one, on the contrary, the performance of FL with end effects are far better than those

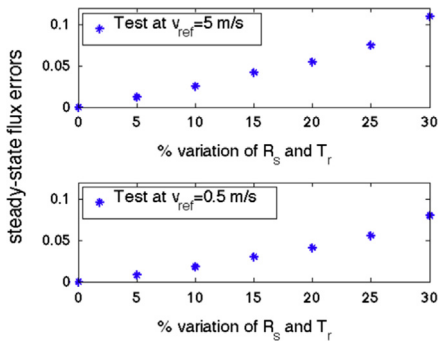

Fig. 14. Steady-state tracking errors of the flux, obtained with FL, versus the percent variations of R_s and T_r during the two speed step references of 0.5 m/s and 5 m/s.

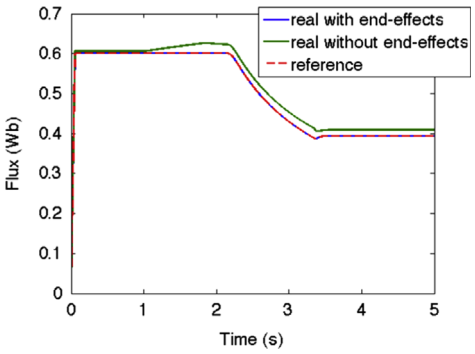

Fig. 15. Reference and measured induced part flux during a speed step from 0 to 10 m/s, with FL with and without end effects.

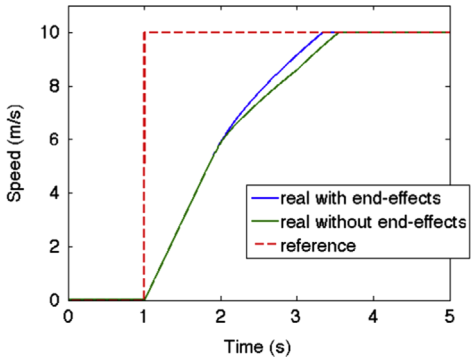

Fig. 16. Reference and measured speed during a speed step from 0 to 10 m/s, with FL with and without end effects.

Table 4
IAE and ITAE control performance indexes obtained with FL not considering the LIM end effects.

Test description	$e_v = v_{ref} - v$	$e_\psi = \psi_{ref} - \psi_r$
Speed reversal $+10$ m/s $\rightarrow -10$ m/s	IAE=52 ITAE=N.A.	IAE=0.332 ITAE=N.A
Test at 0.5 m/s at-load	IAE=0.0170 ITAE=0.0340	IAE=0.0972 ITAE=0.3087

without them, with a resulting speed waveform tracking its reference far more quickly.

Table 4 shows the IAE and ITAE control performance indexes, obtained with FL without end effects, during the same tests shown in Section 2 for the case of FL with end effects. The direct comparison of such indexes, as provided respectively in Tables 2 and 4, highlights that the adoption of FL considering the end effects permits the reduction of such indexes in all cases of at least one order. This implies a significant increase of dynamic performance achievable thanks to the adoption of such FL technique with respect to the corresponding one developed for RIMs. It should be finally noted that the adoption of a LIM with more visible dynamic end effects would imply a higher increase of the dynamic performance with respect to the case under study.

4. Test setup

A test setup has been suitably built to validate proposed FL control technique. The machine under test is a LIM model Baldor LMAC1607C23D99, whose rated data and electrical parameters are shown in Table 1. The LIM has been equipped with a linear encoder Numerik Jena LIA series. The LIM presents an induced part track on length 1.6 m. The employed test setup consists of the following:

- A three-phase linear induction motor with parameters shown in Table 1.
- A frequency converter which consists of a three-phase diode rectifier and a 7.5 kVA, three-phase VSI.
- A dSPACE card (DS1103) with a PowerPC 604e at 400 MHz and a floating-point DSP TMS320F240.

The test setup is equipped also with a torque controlled PMSM (permanent magnets synchronous motor) model Emerson Unimotor HD 067UDB305BACRA mechanically coupled to the LIM by a pulley-strap system, to implement an active load for the LIM.

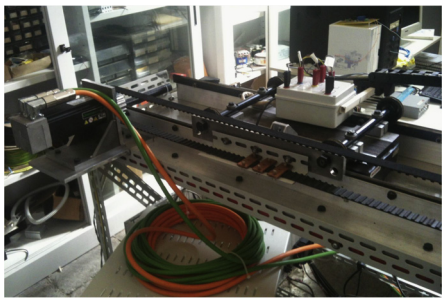

Fig. 17. Photograph of the experimental test setup.

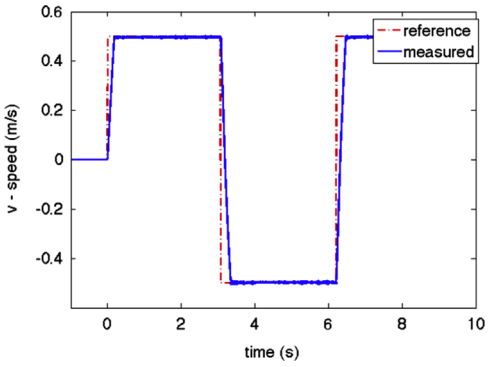

Fig. 18. Reference and measured speed, obtained experimentally, during a square speed reference of 0.5 m/s (FL).

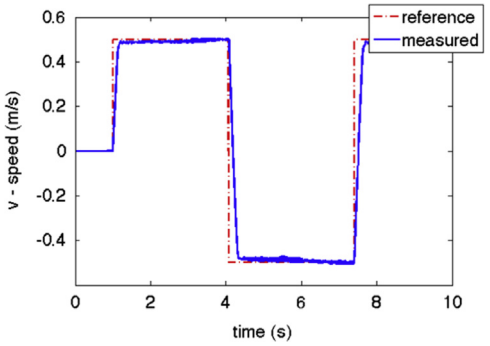

Fig. 19. Reference and measured speed, obtained experimentally, during a square speed reference of 0.5 m/s (FOC).

Table 5
IAE and ITAE control performance indexes for speed error $e_v = v_{ref} - v$, obtained with FL and FOC in the experimental tests.

Test description	FL	FOC
Experimental test at 0.5 m/s, square speed reference	IAE = 0.21 ITAE = N.A.	IAE = 0.26 ITAE = N.A.
Experimental test at 0.5 m/s, at-load	IAE = 1.7×10^{-2} ITAE = 2.3×10^{-2}	IAE = 0.11 ITAE = 0.19

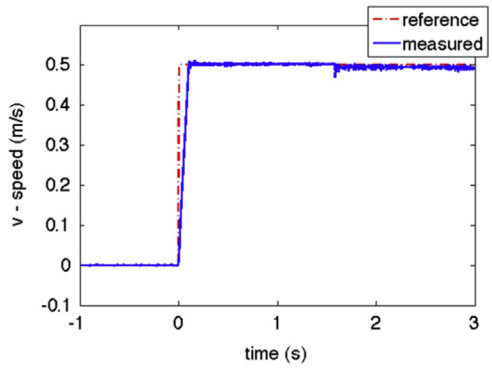

Fig. 20. Reference and measured speed, obtained experimentally, during a step speed reference of 0.5 m/s and with a load of 40 N m applied at 2.5 s (FL).

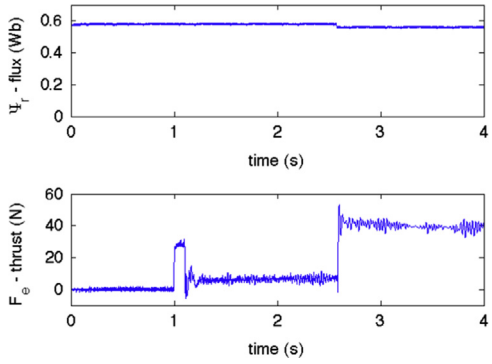

Fig. 21. Estimated induced part flux and electromagnetic thrust, obtained experimentally, during a step speed reference of 0.5 m/s and with a load of 40 N m applied at 2.5 s (FL).

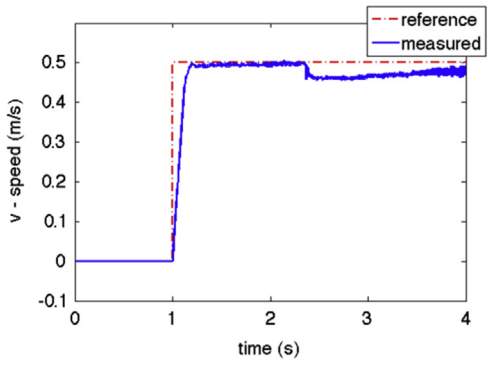

Fig. 22. Reference and measured speed, obtained experimentally, during a step speed reference of 0.5 m/s and with a load of 40 N m applied at 2.5 s (FOC).

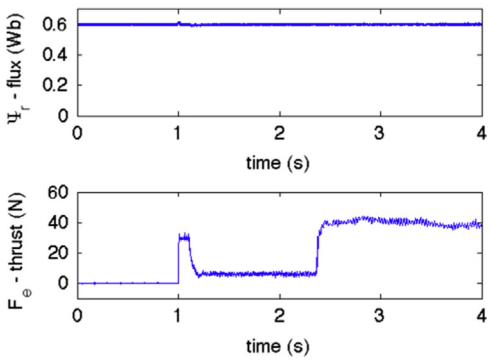

Fig. 23. Estimated induced part flux and electromagnetic thrust, obtained experimentally, during a step speed reference of 0.5 m/s and with a load of 40 N m applied at 2.5 s (FOC).

The computational burden of the FL control algorithm, as implemented on the adopted DS1103 board, has been evaluated in comparison with the corresponding one required by FOC. It has been found that the implementation of FL requires the exploitation of 20% of the sampling time of the control system, whereas FOC requires 15%. The required computational demand is thus only slightly higher.

Fig. 17 shows a photograph of the test setup.

5. Experimental results

As in the simulation results, experimental results have been performed twice, respectively, adopting the proposed input–output feedback linearization technique and adopting the field oriented control. It should be noted that, as for the experiments, tests only at relative low speed could be made because of the limited length of the induced part track. Two kinds of experimental tests have been performed and shown in the following. Firstly the LIM drive, with the machine regularly magnetized at its rated flux, has been given a square speed reference of amplitude 0.5 m/s. The time duration of the square waveform is determined by the length of the track: whenever the LIM gets the end of the track, the inversion of the motion is commanded. Figs. 18 and 19 show the linear speed of the LIM during this test, respectively obtained with the FL and the FOC. The improved dynamic performance achievable with the FL are partially observable at this time scale, while they are confirmed by the IAE performance index shown in Table 5. They show an IAE obtained with FL of 21 while the corresponding one obtained with FOC is 26, confirming an increase of the dynamic performance with FL.

As a second test, the LIM drive has been given a step speed reference of 0.5 m/s at no load. When the LIM is at speed steady-state, a load force of 40 N m is applied at about 2.5 s. Figs. 21 and 23 show the waveforms of the induced part flux amplitude and net electromagnetic thrust, obtained respectively with FL and FOC. Correspondingly, Figs. 20 and 22 show the LIM speed waveforms, respectively obtained with FL and FOC. As for this test, the increase of dynamic performance achievable with FL is clearly visible,

especially with regard to the rejection to the load force application. The response of the speed loop to the load force application is much faster with FL than with FOC. This is confirmed by the analysis of the IAE and ITAE performance indexes, in Table 5. The IAE obtained with FL is 6.5 times lower than the corresponding one with FOC, while the ITAE is 8.3 times lower. These results confirm a net improvement of the dynamic performance achievable with FL.

6. Conclusion

This is the second part of a paper, divided in two parts, proposing the theoretical formulation and the application of the input–output feedback linearization technique to linear induction motor (LIM) drives. This part presents the validation of the proposed FL control technique, taking into consideration the LIM dynamic end effect, in numerical simulation and experimentally on a suitably developed test setup. In particular, a sensitivity analysis on the FL control shows clearly that a variation of both the inductor resistance and induced part time constant is not crucial in regard to the control action. Moreover, simulation results clearly show the improvements achievable in terms of dynamic performance of the control system, adopting the FL formulation which inherently takes into consideration the LIM end effects with respect to that designed for the RIM case. Finally the comparison between the dynamic performance of the LIM drive equipped with the proposed FL control with the corresponding one equipped with the FOC clearly shows significant improvements achievable with the adoption of FL. These improvements are measured by a significant reduction, of the IAE (ITAE) control indexes obtained with FL. Finally, the load rejection capability of the LIM drive with FL control has resulted much higher than the corresponding one with FOC, as highlighted also by the corresponding IAE (ITAE) indexes.

References

Alonge, F., Cirrincione, M., D'Ippolito, F., Pucci, M., & Sferlazza, A. (2014). Parameter identification of linear induction motor model in extended range of operation by means of input–output data. *IEEE Transactions on Industry Applications*, *50*(2), 959–972.

De Luca, A., & Ulivi, G. (1989). Design of an exact nonlinear controller for induction motors. *IEEE Transactions on Automatic Control*, *34*(12), 1304–1307.

Kim, D.-I., Ha, I.-J., & Ko, M.-S. (1990). Control of induction motors via feedback linearization with input–output decoupling. *International Journal of Control 51*(4), 863–883.

Krzeminski, Z., (1987). Nonlinear control of induction motor. In *10th IFAC World Congress* (Vol. 349, p. 33), Munich.

Leonhard, W. (2001). *Control of electrical drives*. Berlin: Springer.

Marino, R., Peresada, S., & Valigi, P. (1993). Adaptive input–output linearizing control of induction motors. *IEEE Transactions on Automatic Control*, *38*(2), 208–221.

Marino, R., Tomei, P., & Verrelli, C. M. (2010). *Induction motor control design*. London: Springer.

Pucci, M. (2012). Direct field oriented control of linear induction motors. *Electric Power Systems Research*, *89*, 11–22.

Pucci, M. (2014). State space-vector model of linear induction motors. *IEEE Transactions on Industry Applications*, *50*(1), 195–207.

Vas, P. (1998). *Sensorless vector and direct torque control*. Oxford, UK: Oxford University Press.